BUILD SIMUL (2015) 8: 353 – 366
DOI 10.1007/s12273-015-0214-y

Design of optimal building envelopes with integrated photovoltaics

Amr M. A. Youssef[1,2], Zhiqiang (John) Zhai[1] (✉), Rabee M. Reffat[2]

1. Department of Civil, Environmental and Architectural Engineering (CEAE), University of Colorado, UCB 428, ECOT 441, Boulder, CO 80309, USA
2. Architecture Department, Assiut University, Assiut 71518, Egypt

Abstract

Building integrated photovoltaics (BIPV) receives growing attentions due to both architectural and engineering favorability. Large commercial building envelopes present a great potential of utilizing solar radiation, especially in climate zones with rich solar resources. Most current studies have been focused on predicting and optimizing power generation of BIPV on designed envelope systems, which leaves limited room for performance improvement of BIPV. This study introduces a framework of an optimization method that formulates the best building envelope shapes and the most matching BIPV systems. A set of criteria are established to determine the best alternatives of envelope variations, upon which the power generation and economic impact of different BIPV systems are evaluated and compared. The proposed optimization process was demonstrated using a general commercial building design application in Egypt. The developed tool can help designers in achieving an optimized building envelope that is most suitable for PV integration.

Keywords

building integrated photovoltaics,
optimal building envelope,
power generation,
economic analysis

Article History

Received: 5 August 2014
Revised: 6 January 2015
Accepted: 8 January 2015

1 Introduction and background

About 21% of the world electricity in 2011 was generated from renewable energy, with a projection of increase to nearly 25% in 2040 (EIA 2013). Hence, global efforts are put to create reliable solutions for utilizing renewable energy on site at buildings. Photovoltaic (PV) systems are promoted and used widely in electrifying buildings as a sustainable technique. Due to the limited space on the roof, additional solar-accessible areas (such as external facades) are needed to provide necessary electricity for building applications. ASHRAE standard specifies the consumption of a commercial building to be 13.4 kWh/(ft^2·yr) in hot climates (ASHRAE 2007), while it is estimated that roof-mounted PV can generate 40.4 kWh/(ft^2·yr) in standard test conditions[1]—merely supply 3 floors of electricity. Integrating PV with building facades provides more architectural dynamics and thus receives more attention recently from the architectural perspective.

The major challenges for building integrated PV (BIPV) design and application are relatively higher cost and lower efficiency, mostly due to un-ideal position towards the solar exposure. The problems, however, may be addressed if building forms can be reshaped for optimal PV energy and economic performance—the goal of this study. For example, tilting a vertical southern facade to increase the solar zenith angle by 15 degrees may increase 32% generation power in hot climates, predicted using Autodesk ECOTECT (Autodesk 2014). This study proposes a framework of an optimization method that formulates the best building envelope shapes as well as the most matching PV modules to be attached, using the power generation rate and the economic impact as two optimization criteria. The more specific goals include:

1) identifying the best envelope designs that have most solar exposures;
2) finding the most applicable and cost-efficient PV systems for the optimal envelopes.

The developed optimization process was demonstrated using a typical commercial building in Egypt, which represents one of the most common envelope shapes of commercial buildings in Egypt.

E-mail: john.zhai@colorado.edu

[1] Standard test conditions: 1000 watts per square meter of sunlight intensity, hold a cell temperature of 25℃ and assume an air mass of 1.5 (AM Solar 2014).

List of symbols

BIPV	building integrated photovoltaics	S_{An}, S_{Bn}, S_{Cn}, S_{Dn}	n is the serial number of an integration option for (S_A, S_B, S_C, S_D)
SAM	System Advisor Model (a software tool)	$S_{A'n}$, $S_{B'n}$, $S_{C'n}$, $S_{D'n}$	n is the serial number of integration option to be applied on ($S_{A'}$, $S_{B'}$, $S_{C'}$, $S_{D'}$)
RETScreen	Renewable Energy Technologies Screen (a software tool)	PVi	i is the PV module number in the conducted PV database (as shown in the appendix)
WWR	window-to-wall-ratio	Alt i	i denotes the number of a main alternative of the base model, these alternatives are generated by applying orientation variations
S	one of the model surfaces	Alt i–i'	i' denotes the number of a secondary alternative of the optimized model, which is generated from the main alternative Alt i
S_A, S_B, S_C, S_D	"A", "B", "C" and "D" refer to roof, southern, eastern and western facade surfaces in the model respectively		
$S_{A'}$, $S_{B'}$, $S_{C'}$, $S_{D'}$	these surfaces refer respectively to (S_A, S_B, S_C, S_D) after varying their orientation (e.g. S_A will be $S_{A'}$ if an orientation variation was applied for optimization)		
$S_A \rightarrow S_{A'}$	applying an orientation variation (change the orientation) on S_A to be converted to $S_{A'}$		

A few papers were focusing on optimizing building envelope for more energy consumption efficiency. Karaguzel et al. (2014) proposed an integrated energy simulation and multi-dimensional technique to minimize life cycle cost via the envelope design of a commercial building; the technique results are the optimal values of thermal insulation thicknesses of envelope components. You et al. (2013) proposed an integrated approach to evaluating facade design influence on daylighting, thermal performance and natural ventilation. Tuhus-Dubrow and Krarti (2010) developed an approach to optimizing envelope properties of residential building via selecting optimal values from envelope parameters. Few studies were aiming to optimize PV installation to maximize its electric current generation. Hwang et al. (2012) presented an analytic optimization for PV module inclinations and related spacing distances between them in office building facades. Choudhary et al. (2008) proposed a design analysis process for obtaining a functional net-zero energy solar house using PVs. Efforts to optimizing both the power generation and the building energy use were not found in the literature.

Approaches and tools were developed to help achieve best building geometries with high solar energy impact. For instance, computational tool "RADIANCE" can assist to optimize urban geometric forms for the solar irradiation utilization (Kampf and Robinson 2010). Sui and Munemoto (2007) developed a simulation program "GRIPVS" to study the optimal gable roof shape with lower CO_2 emission and higher investment value. These studies, however, do not provide detailed building envelope alternatives that can maximize PV performance. "SOLVELOPE" program can generate 3D envelope shapes to meet annual heating needs from solar energy for a given site (Topaloğlu 2003; Capeluto et al. 2005). Jin et al. (2012) proposed an optimization algorithm using "RHINO" program to minimize building thermal load. These studies focus on site and building thermal loads, respectively, but not BIPV. No study was found in literature that suggested an approach to formulating optimal building envelope shapes and the appropriate PV systems for the identified envelopes. This paper proposes a framework of such an approach.

2 Proposed optimization framework

The proposed optimization framework (Fig. 1) consists of two principal steps as detailed below.

2.1 Step 1: Optimization of the building model based on sensitive analyses of solar exposure on all surfaces

The required inputs for this optimization are: initial building shape, building height, orientation, location (climate identification), forms of surrounding buildings and the spaces between them (streets). The initial shape can be selected from a list of the common simple building shapes (square, rectangle, L shape, etc.) or can be drawn from the scratch if the building has a different shape, and its dimensions can be specified or converted accordingly to (x, y, z) values for the outline dimensions, ($x1$, $y1$, etc) values for internal dimensions if required (e.g. U shapes) and ($w1$, $w2$, etc) for

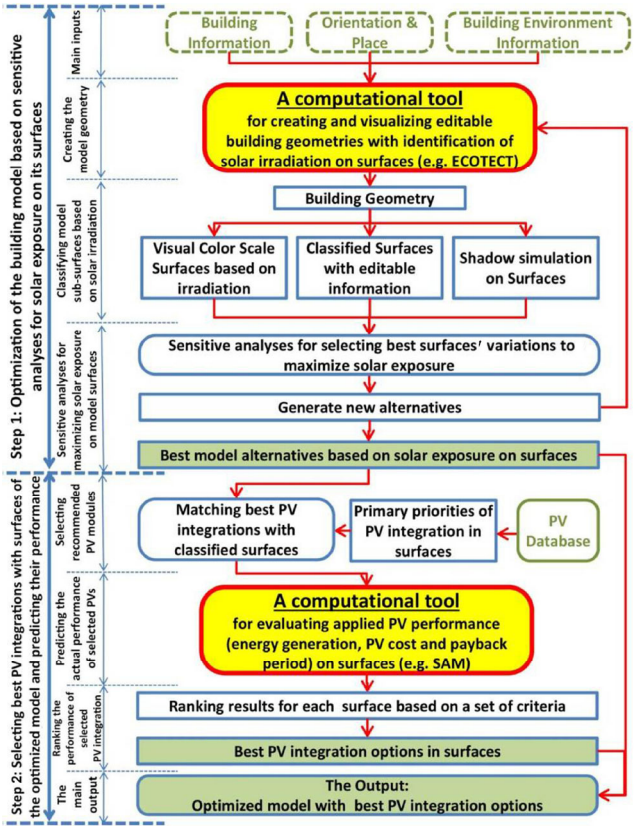

Fig. 1 The proposed optimization framework

widths of different surrounding streets. Accordingly, 3D models can be developed and visualized using Autodesk ECOTECT (Autodesk 2014), Open studio Sketch Up plug-in (Open Studio 2014) and others to allow the calculation of: (a) solar exposure: e.g., visual color scales, to evaluate various model surface variations; (b) shadow: to evaluate the shading effect on building surfaces; and (c) surface classification: e.g., roofs, walls, windows, etc, to evaluate the related impact on solar exposure at surfaces. Building orientation can also be altered and tested for all facades towards an optimal solar exposure solution. This can provide more PV modules with less space requirements and costs, than merely orienting PV modules towards the sun.

Sensitive analyses are performed to determine the most sensitive surface variations so as to maximize solar exposure. Figure 2 shows an example of generic irradiation values (kWh/(m^2·yr)) for different orientations (every 15 degrees). These values are related to the international hot climate zone (2A), as an example, based on ASHRAE 90.1 standard[2].

[2] ASHRAE 90.1 standard defines and classifies the international climate zones using letters and numbers; letters (A), (B) and (C) refer to moist, dry and marine climate zones, respectively, while numbers (from 1 to 8) refer to the temperature (from the hottest to the coldest climate zones), respectively (ASHRAE 2007).

Maximum surface tilt is set at 120 degrees to avoid less solar exposure on surfaces beyond that angle. Building surfaces can then be varied in steps towards the orientations that improve solar exposure. These orientation variations can be classified as: (a) main orientation variations: the most sensitive variations in improving solar exposure on a given surface and (b) secondary orientation variations: all other improving variations.

Applying these variations in separated steps leads to optimized alternatives with more solar exposure on each surface, and further different building mass volume and area of surfaces. Applying more variations in one step, however, may lead to an impractical architectural massing for a given design. Solar exposure rate per cubic meter, rather than the absolute solar exposure, is used as the ranking indicator for evaluating the alternatives, because alternatives with more volume have more solar exposure on their surfaces, but also will contain more spaces/volumes that require more energy consumption. In addition, the minimum required architectural area for a building should be considered to avoid function inadequacy in alternatives. The standard required occupying area for offices is 18 m^2/person in large office buildings (Baiche and Williams 2001) (ASHRAE 2007), while the architectural minimum area requirement is 12 m^2/person (Baiche and Williams 2001). The best building alternatives should have more solar exposure rate per cubic meter than the initial model, but not having less than the minimum required architectural area.

These variations can be applied to both simple and complex cubic building shapes, as illustrated in Fig. 3. More complex buildings, such as free-form shape designs or curved envelopes, are not applicable in this optimization method. Such shapes require other concepts such as the "shape grammars" concept to refine different geometry alternatives of each facade. Shape grammars perform computations for shapes by a recognition of a particular shape and its possible replacements using various developed rules (Gips 2012).

The step-1 achieves a 3D optimized model with more solar exposure on all of its surfaces.

2.2 Step 2: Selecting the best PV integrations with the optimized surfaces and predicting their performance

Different surfaces (roofs, walls, windows, etc.) in the optimized building have different PV integration alternatives. External facade can be integrated as a solid wall with opaque PVs or windows with semi-transparent PVs. Hence, a classified PV database is needed to cover all surface types,

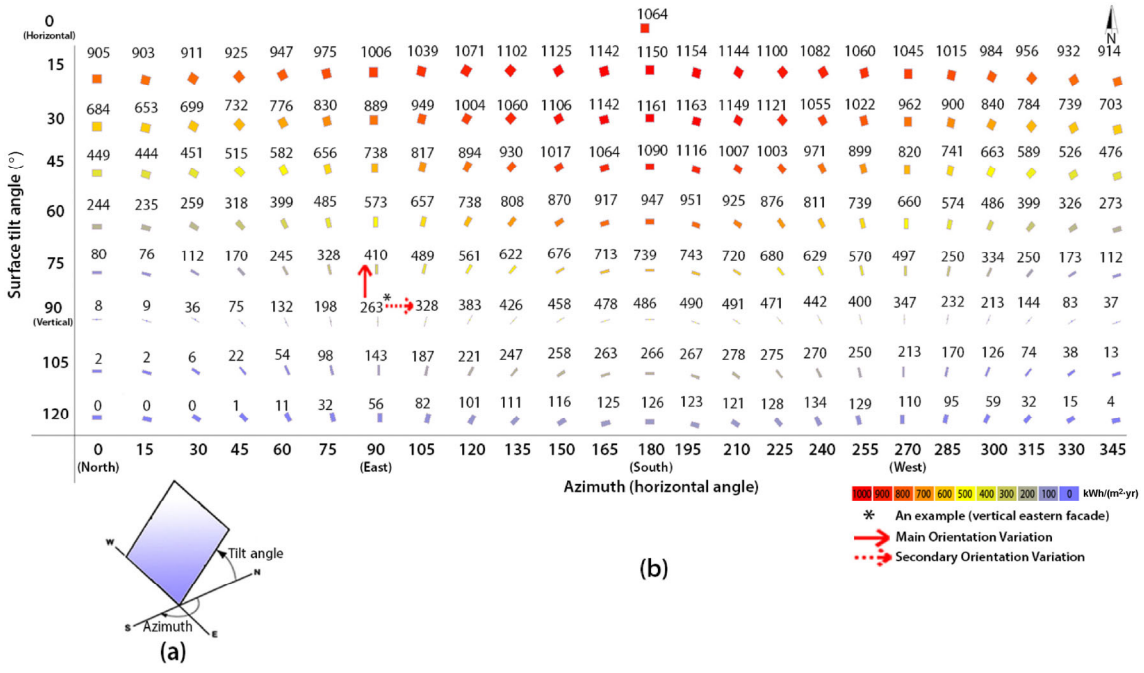

Fig. 2 Irradiation values on different oriented surfaces: (a) azimuth and tilt angle specification; (b) irradiation values and related orientation variations

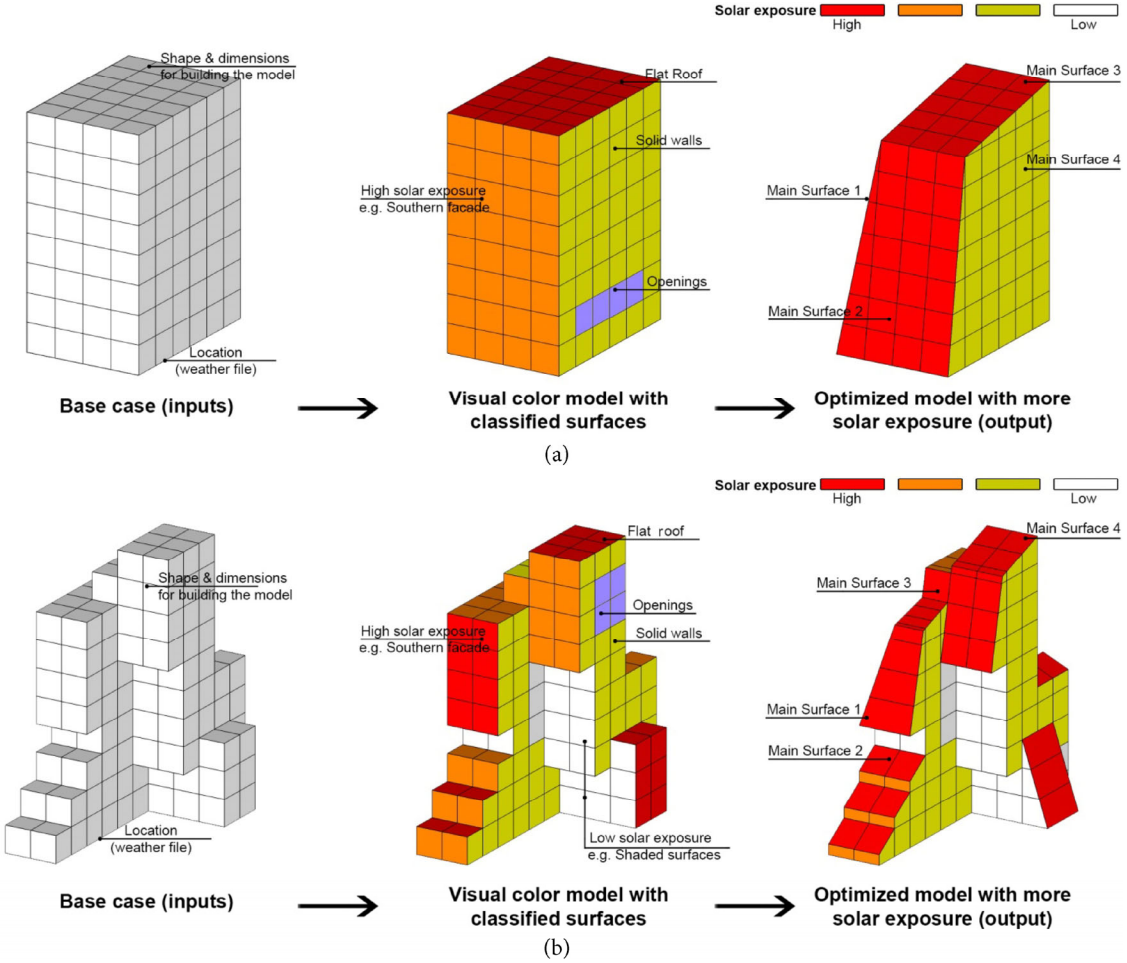

Fig. 3 The inputs and outputs in Step 1: (a) simple cubic buildings; (b) complex cubic buildings

in which the generation capacity and cost of generation are two main classification parameters. Cost of generation includes costs of PV modules, required equipments and installation, but not maintenance cost. PV cost payback period can be used as a parameter to exclude some integrations, assuming the payback period should not exceed the PV lifespan (25 years in average). Table 1 presents general applicability recommendations between the classifications of PV and surfaces. This applicability is not affected by location (climate zone), building type, architectural preference and others, although these criteria will affect PV performance in general. The table was produced using many resources (e.g., Ly et al. 2013; SFA 2013; Kho 2010; Harvey 2009; Albere 2009; Henemann 2008; Gumm 2008; Suna et al. 2006; Prasad and Snow 2005; Carmody et al. 2004). Actual performance of recommended and applicable PV modules for each surface type can be ranked based on energy generation and cost using tools such as SAM (NREL 2014), RETScreen (NRCAN 2014) or eQuest (DOE-2 2014).

The final output from this step-2 is the determination of the most matching PV modules that can be integrated on various surfaces of the optimized building, whose actual performance will be predicted. Designers can then select one of the best solutions according to their project priorities.

Table 1 Applicability recommendations between the classifications of PV and surfaces

				Surface classification														
				Roofs				Facade										
										Windows				Orientation				
				Flat roofs	Tilted roofs	Skylight	Curved surfaces	Solid walls	Shaded areas	For view	For daylight	Curtain walls	Shadings	South	West	East	Atrium
PV classification	PV type	Mono-crystalline silicon PV												■			
		Poly-crystalline silicon PV												■			
		Amorphous thin film PV							■	■	■	■					
	Additional tech.	Tracking systems											■	■			
		Concentrated PV modules			■	■	■	■	■	■	■	■					
	Transparency	Transparent A-Si PV glazing(thin film)	>30%	■	■			■		■							
			<30%	■	■	■		■	■	■			■		■	■	
		Semi-transparent PV (on glass)	>30%	■	■			■		■	■						
			<30%	■	■	■		■	■		■		■		■	■	
		Opaque PV	0%			■		■		■	■	■	■				■
	Flexibility	Flexible PV modules		■	■												
		Foldable PV modules															
		Non-flexible PV modules		■	■			■									
	Reflection	Reflective PV modules							■			■		■			
		Semi-reflective modules													■	■	
		Non-reflective modules												■			
	Cost	High PV cost								■	■	■					■
		Low PV cost		■	■								■				

■ Recommended application ■ Applicable integration ■ Not recommended application ■ Not applicable

3 Application of the proposed framework for a pilot project

A pilot commercial building application in Egypt is demonstrated using the proposed framework. Egypt has hot climatic conditions with good solar resources which can maximize PV technique impacts, and 90% of electrical power generation in 2010–2011 in Egypt came from fossil fuels (Ministry of Electricity and Energy 2011). A representative sample of 25 office buildings in Cairo were collected and analyzed to determine the base building model as illustrated in Fig. 4. It reveals that the majority of office buildings have a cuboid form, a square plan, and their floor average area equals approximately 2564 m^2.

As a result, the pilot building is constructed with the 1:1:2 form ratio (width: length: height), 2500 m^2 area and 100 m height (25 story). An office complex of the same building design is used to demonstrate the surrounding building impacts. Considered surfaces include: roof (S_A), southern (S_B), eastern (S_C) and western (S_D) facades as illustrated in Fig. 5. The optimization constraints for this application are: (a) alternatives cannot exceed the building volume (50 m × 50 m × 100 m), (b) the north facade is ignored due to its lack of solar exposure and (c) window-to-wall-ratio (WWR) is fixed at 40% for all facades to minimize the number of alternatives for this demonstration. The proposed optimization procedure is implemented on the model, as detailed below.

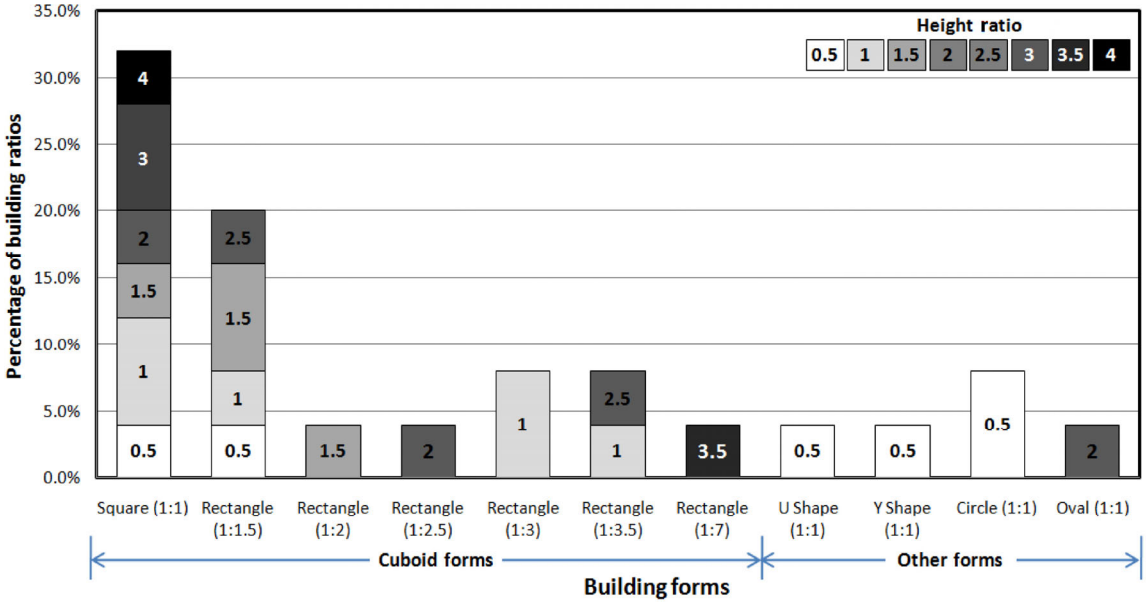

Fig. 4 The ratio of different building forms in Egypt (Cairo)

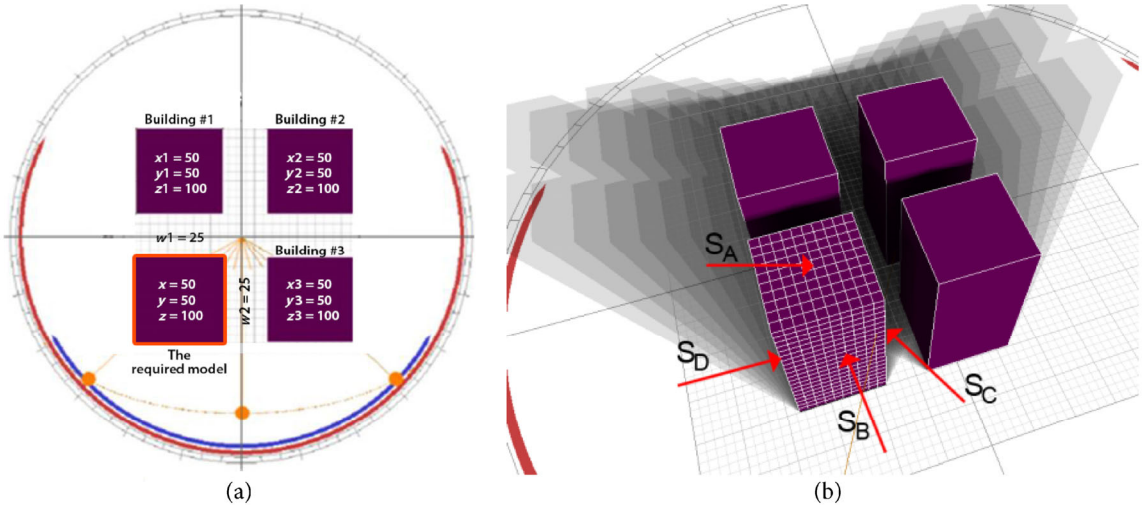

Fig. 5 The pilot model features: (a) layout and dimensions; (b) considered surfaces on the model

3.1 Optimization of the building based on sensitive analyses for solar exposure on surfaces

3.1.1 Main inputs

Main inputs are: dimensions of the required model (50 m × 50 m × 100 m), its surrounding buildings (with the same volume), streets' widths (25 m each) and location (using Cairo weather file).

3.1.2 Creating the building geometry

Accordingly, the building model geometry can be created or input in ECOTECT.

3.1.3 Classifying model sub-surfaces based on solar irradiation

Figure 6 illustrates the obtained 3D visual color scale, the irradiation value on all geometry sub-surfaces (5 m × 5 m) and sub-surface classification by type (e.g. wall, window or etc).

3.1.4 Sensitive analyses for maximum solar exposure on model main surfaces

The solar exposure on main surfaces (facades) can be improved by applying the orientation variations with their classification (main and secondary) as illustrated in Fig. 2 on each main surface. Table 2 illustrates the different improvements in solar exposure on each main surface after applying the available orientation variations respectively. Based on the sensitivity test for improvements, 3 main and 3 secondary orientation variations are sensitive. The main orientation variations are to tilt the vertical eastern, southern and western facades, respectively, to increase the solar zenith angle by 15 degrees. The secondary orientation variations are to tilt the horizontal surface to face the south, increasing the azimuth angle of the eastern facade and reducing the azimuth angle of the western facades, respectively, by 15 degrees. Figure 7 illustrates applying the main variations first; different combinations of the 3 main orientation variations will generate 7 main model alternatives (Alt 1 to Alt 7). Then, 3 secondary variations can be applied to

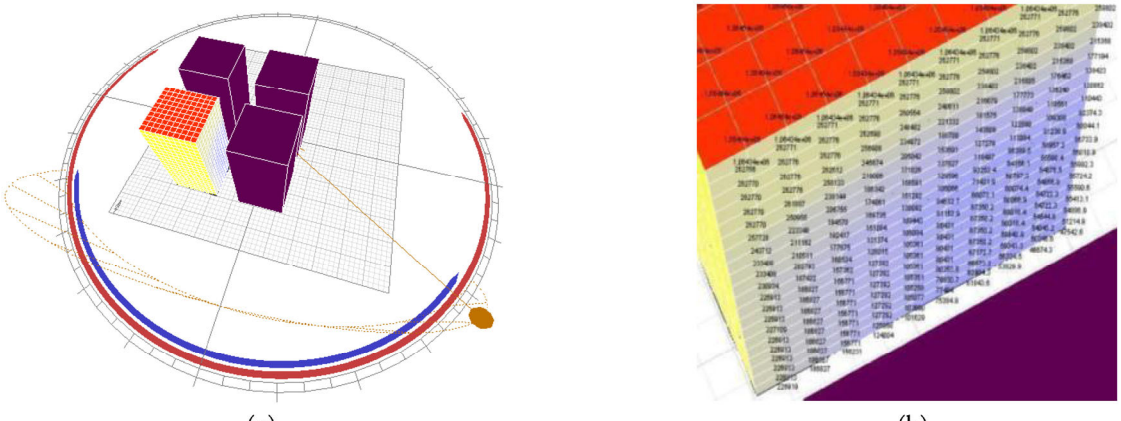

(a) (b)

Fig. 6 The model geometry (ECOTECT output): (a) visual color scale model; (b) solar irradiation values on all model subsurfaces of 5 m × 5 m

Table 2 Solar exposure improvements on each model facade by applying orientation variations and classifying them

	Main orientation (azimuth, surface tilt)→irradiation (kWh/(m²·yr))	Available optimized orientations (azimuth, surface tilt)→irradiation (kWh/(m²·yr))	The additional improvements (percentage)	Classification of orientation variation (main/secondary)
S_A	(0, 0)→ 1064	(0, 15)→ 1150	+ 8.1%	Secondary
S_B	(180, 90)→486	(180, 75)→739	+52.1%	Main
		(195, 90)→ 490	+0.8%	Secondary
S_C	(90, 90)→263	(90, 75)→410	+55.9%	Main
		(105, 90)→328	+24.7%	Secondary
S_D	(270, 90)→347	(270, 75)→497	+43.2%	Main
		(255, 90)→400	+15.3%	Secondary

Note: shaded improvements are not sensitive.

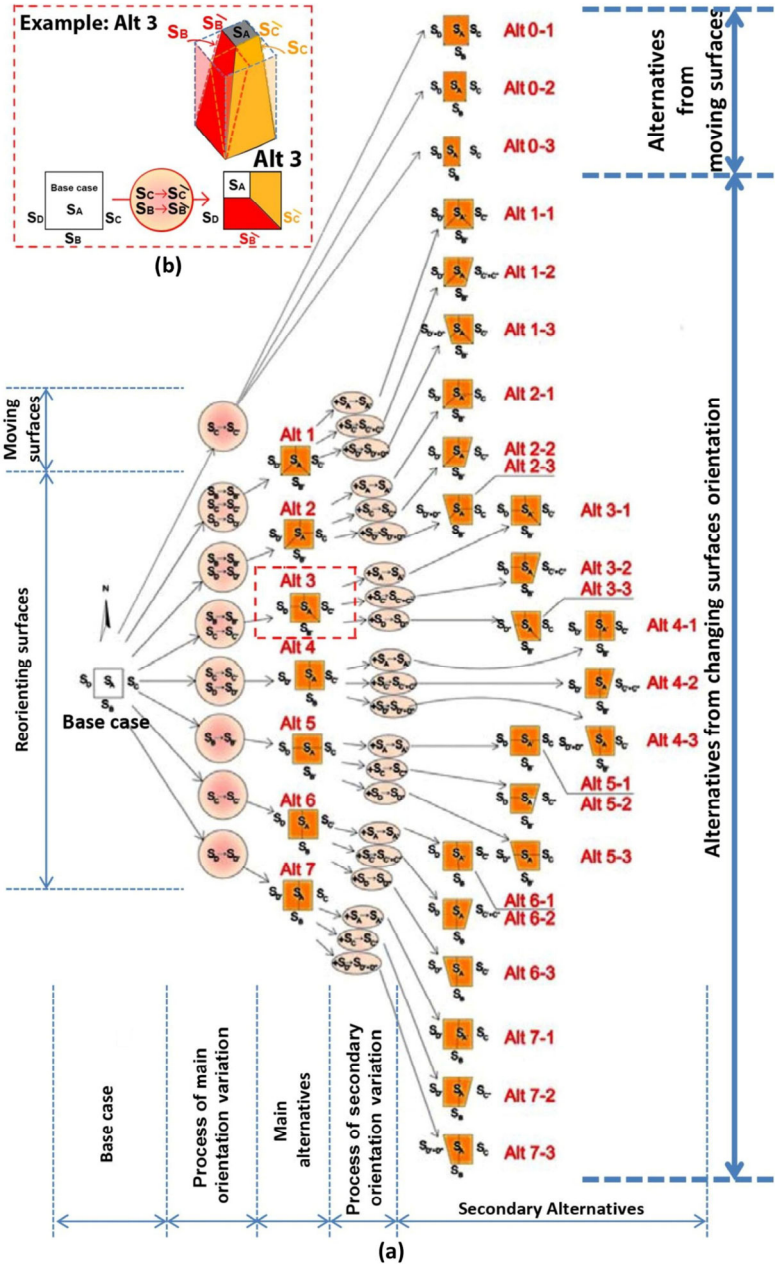

Fig. 7 Generated alternatives to optimize the initial model: (a) generation tree, (b) an explanation exampled (Alt 3)

generate secondary alternatives from main ones (Alt 1–1, Alt 2–1, etc). Due to the relatively lower sensitivity of secondary variations in this application, they will be applied independently without considering their combinations. Moving surfaces (each 10 m) are also studied, and only the eastern facade can optimize the solar exposure to avoid shadows from surrounding neighbors. This provides 3 other alternatives (Alt 0–1, Alt 0–2, Alt 0–3).

Solar exposure on the obtained alternatives (32 alternatives) is simulated and ranked using ECOTECT. Based on the standard required area for offices (18 m^2/person) and the architectural minimum occupying area (12 m^2/person), the floor areas in the pilot building (2500 m^2) can be reduced to 1666.67 m^2 in average after the optimization in order to house the same number of occupants in the designed building. With the same number of stories and their heights, the minimum volume of the optimized alternatives is 166 666.67 m^3 (1666.67 m^2 × 100 m). Alternatives less than that volume are avoided as illustrated in Table 3. In this application, the highest solar exposure is achieved in alternatives Alt 5–1 and Alt 5 (shown in Fig. 8); Alt 5 has more absolute solar exposure, larger volume and less solar exposure per m^3 than Alt 5–1. Alt 5 is presented in the following application.

Table 3 Ranking of all optimized alternatives based on solar irradiation and mass volume

	Radiation on different surfaces (MW/yr)						Ranking parameter	
Alternative number	S_A	S_B	S_C	S_D	Others	Total	Volume (m^3)	Total radiation ($kWh/(m^3 \cdot yr)$)
Base case	2661.6	2433	849.5	1736.9	—	7681	250000	30.7
Alt 0–1	2129.3	1948.6	980.3	1736.9	—	6795	200000	34.0
Alt 0–2	1596.9	1461.8	1111.5	1736.8	—	5907.2	150000	39.4
Alt 0–3	1064.6	970.6	1196.5	1736.9	—	4968.6	100000	49.7
Alt 1	—	1767.4	831.3	1803.9	—	4402.5	97188.8	45.3
Alt 1–1	—	1767.4	831.3	1803.9	—	4402.5	97188.8	45.3
Alt 1–2	—	1571.5	229	758.4	1803.9	4362.7	92786.2	47
Alt 1–3	—	1572.4	1084.5	1295.6	409.5	4362	92785.6	47
Alt 2	573.2	2020	547.2	1887	—	5027.6	139957.7	35.9
Alt 2–1	718.7	2640.1	487.6	1843.3	—	5689.7	138107.6	41.2
Alt 2–2	496.8	2020.5	785.5	1887.1	—	5190	121206.9	42.8
Alt 2–3	573.6	2561.1	547.2	1380.7	409.5	5472.3	135555.1	40.4
Alt 3	573.2	2787.1	1166.4	1267.9	—	5794.6	139957.7	41.4
Alt 3–1	718.7	2661.5	1096.96	1241.2	—	5718.3	138107.6	41.4
Alt 3–2	573.2	2579.9	879.6	229.3	1268.2	5530.3	135555.1	40.8
Alt 3–3	389.9	2043.5	1166.4	1524.8	—	5124.8	121206.9	42.3
Alt 4	—	1131.7	1544	2405.1	—	5080.9	116626.6	43.6
Alt 4–1	53.5	1133.7	1477.5	2361.9	—	5026.7	116526.4	43.1
Alt 4–2	—	969.2	296.2	1145	2405.2	4815.6	111062.4	43.4
Alt 4–3	—	969.5	1544	1760.7	520.7	4794.9	111052.7	43.2
Alt 5	1233.3	3754.8	547.2	1267.9	—	6803.3	183012.7	37.2
Alt 5–1	1488.8	3509.3	486.8	1241.3	—	6726.3	179126.6	37.6
Alt 5–2	1156.6	3065.8	784.7	1268.2	—	6275.4	164262.9	38.2
Alt 5–3	1156.6	3009.5	547.2	1524.8	—	6238.2	164262.9	38
Alt 6	1234.9	1782.9	1690.6	1732	—	6440.5	183012.7	35.2
Alt 6–1	1491.2	1619.9	1496.6	1616.2	—	6223.9	174893.7	35.6
Alt 6–2	1235	1610.6	1287.2	314.2	1732.2	6179.4	177361	34.8
Alt 6–3	878.5	1126	1690	2082.9	—	5778.2	149519.1	38.6
Alt 7	1234.9	1782.9	1633	1793	—	6443.9	183010.4	35.2
Alt 7–1	1491.2	1619.9	705.3	2405.4	—	6221.9	174840.7	35.6
Alt 7–2	878.5	1126.2	1192.6	2578.1	—	5775.4	149519.1	38.6
Alt 7–3	1235	1613.8	849.9	520.7	1933.4	6152.9	177430.4	34.7

Note: shaded alternatives have less volume than the required minimum.

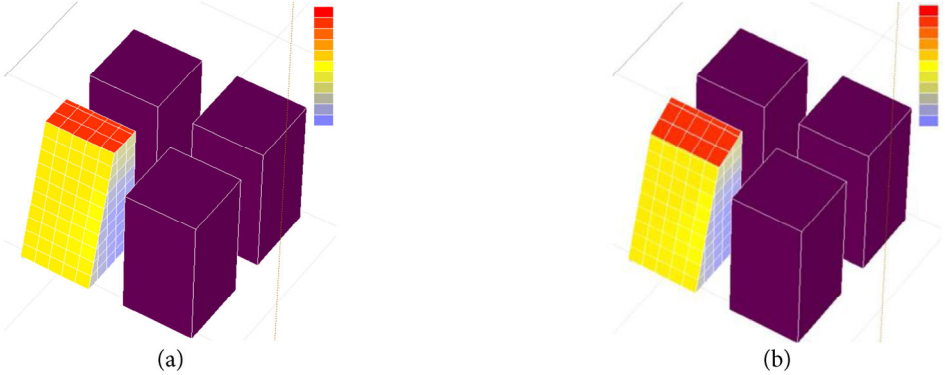

(a) (b)

Fig. 8 Best optimized alternatives based on solar exposure and volume: (a) Alt 5; (b) Alt 5–1

3.2 Selecting best PV integrations with surfaces of the optimized model and predicting their performance

3.2.1 Selecting recommended PV modules to be integrated with corresponding surfaces

Each sub-surface in the optimized model has many available options to be supplied with PV. Figure 9 illustrates the classification of each surface and the related PV integration options. Surfaces are classified based on type, tilt and shading effect (the effect of neighbors in shading the optimized model surfaces), while integration options are classified based on type, required transparency and mobility. For instance, S_A represents a sunny horizontal roof that can be integrated with PV as a movable or fixed semi-transparent skylight or fixed solid roof.

A database of 67 PV modules was collected from manufacturers (shown in the appendix) to be matched with each surface option. Table 4 illustrates the PV integration recommendations for each surface option ranked based on the generated energy (W/m^2) and cost of generation ($/(W·yr)); these recommendations were extracted from Table 1. For instance, PV48 is not applicable on S_{A1} (semi-transparent skylight) since it is an opaque module.

PV modules with higher generated energy and lower cost are selected from recommended and applicable modules for each surface option as shown in Table 5. This prior selection insures technically suitable integration before predicting the actual performance.

3.2.2 Predicting and ranking the actual performance of selected PVs on corresponding model surfaces

Using SAM tool, PV performance can be predicted and ranked based on the actual energy generation, cost of generation, capital cost and payback period as shown in Fig. 10. Options with longer payback periods than PV lifespan (25 years in average) are excluded (PV41 on S_{D3} and

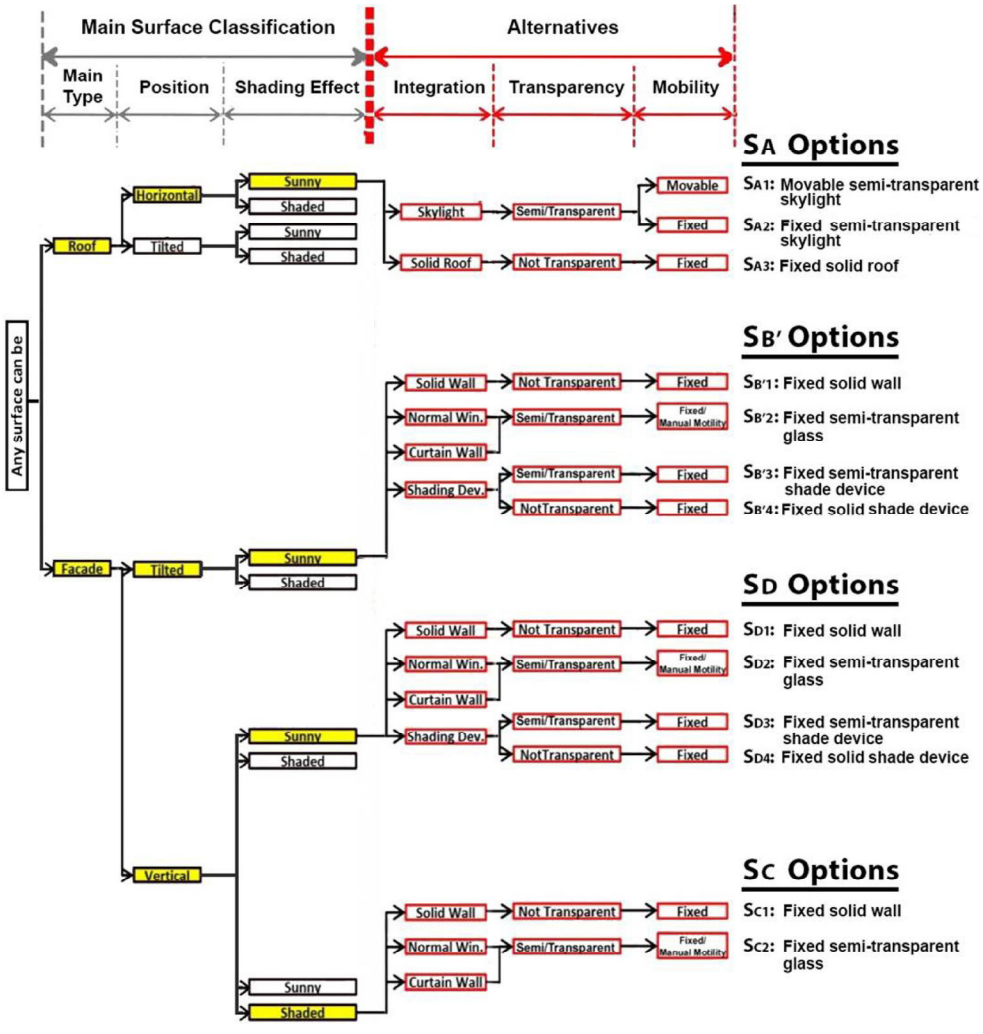

Fig. 9 Classifications and integration options for each surface of the optimized model (highlighted items in the main surface classification represent the application of the model surfaces)

Table 4 PV integration recommendations for each surface: (a) ranked based on generated energy (W/m²); (b) ranked based on cost ($/(W·yr))

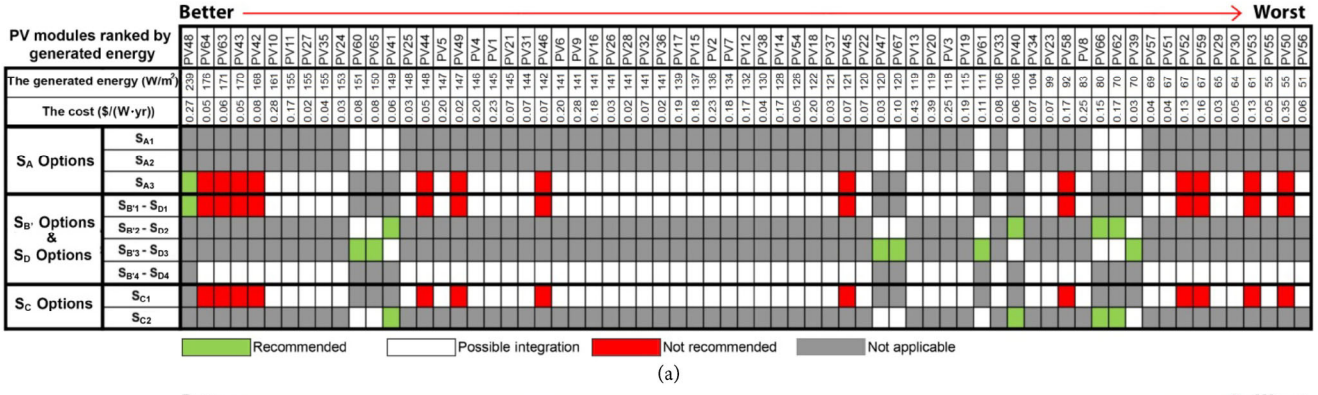

Table 5 Selecting PV modules with higher generated energy and lower cost for each surface option

	Recommended and applicable PV modules for each surface option	
	Energy generation ranking	Economic ranking
S_{A1}, S_{A2}	PV60 – PV65 – **<u>PV41</u>**	PV39 – PV47 – **<u>PV41</u>** – PV40
S_{A3}, $S_{B'1}$, S_{D1} , S_{C1}	PV48 – PV10 – PV11 – **<u>PV27</u>** – PV35	PV36 – **<u>PV27</u>** – PV28 – PV29 – PV 37
$S_{B'2}$, $S_{B'3}$, S_{D2} , S_{D3} , S_{C2}	PV60 – PV65 – **<u>PV41</u>**	PV39 – PV47 –**<u>PV41</u>** – PV42
$S_{B'4}$, S_{D4}	PV64 – PV63 – PV43 – PV42 – PV10 – PV11 – **<u>PV27</u>**	PV36 – PV49 – **<u>PV27</u>** – PV28 – PV29

Note: bold and underlined PV modules are selected.

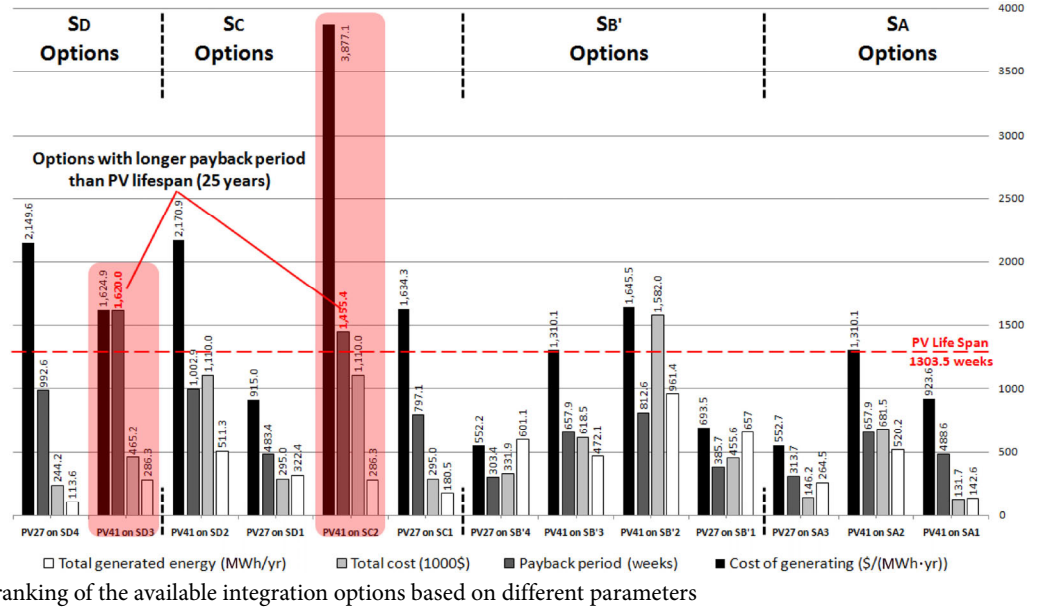

Fig. 10 The ranking of the available integration options based on different parameters

PV41 on S_{C2}); the remaining are the best integration options for the specified surfaces. Designers can select among these options based on their project priorities. For example, if maximizing energy generation is the first priority, the best solution is applying (PV41) with a fixed skylight on the roof, (PV27) with solid wall of eastern facade, and/or (PV41) with the glass of southern and western facades. The best economic solutions are to: applying (PV27) on the solid roof, the southern shading devices, and the western solid wall.

3.2.3 *The application outcome*

The ultimate application output is an optimized building envelope with the most matching PV integration options based on energy generation and cost as illustrated in Fig. 11. This application outcomes also verifies the viable of applying the proposed method for optimizing a given building geometry with BIPV potentials.

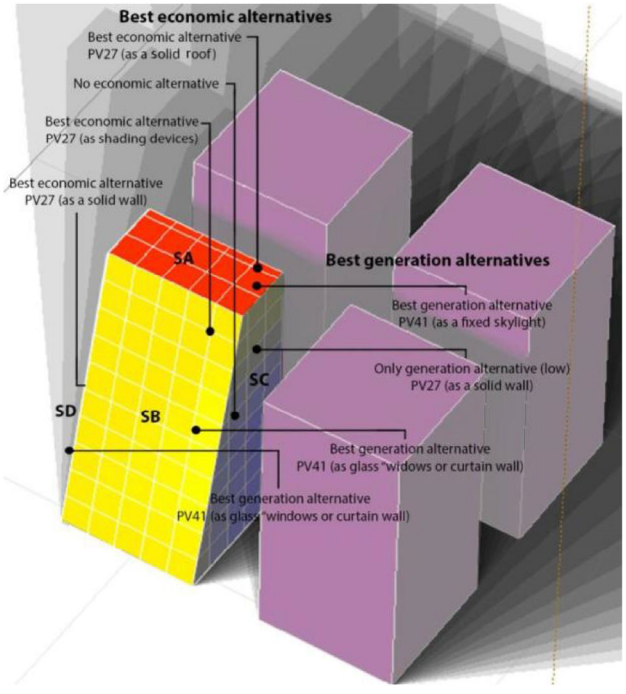

Fig. 11 The ultimate application outcome

4 Conclusions

This paper presents a framework of an optimization method that formulates the best building envelope shapes and the most matching BIPV systems. An initial building shape in a specific environment and the related dimensions are required to start the framework steps. Accordingly, a 3D model can be developed using Autodesk ECOTECT to simulate solar exposure on model surfaces. Sensitive analyses can determine the most sensitive orientation variations to improve solar exposure. Building surfaces can then be varied towards these sensitive orientations to generate optimized alternatives. Alternatives, which meet the minimum floor area requirement, will be ranked based on solar exposure. Surfaces of optimized alternatives can have different PV integration options. The most matching PV modules can be integrated on various surfaces of the optimized building, whose actual performance can be predicted. The PV generation capacity and cost of generation are two main classification parameters in this optimization.

A general commercial BIPV building design in Egypt was demonstrated using the proposed approach. A representative sample of 25 office buildings in Cairo was analyzed first to determine the general base building model. The most sensitive surface variations were applied on the base model to generate alternatives. As a result, the best alternative receives 37.2 kWh/(m^3·yr) solar irradiation while the base model receives 30.7 kWh/(m^3·yr). Surfaces of the optimized model were classified based on the related PV integration options. A database of 67 PV modules was collected to be matched with surface options and the best PV module for each surface was determined. Using the SAM tool to predict PV performance, the best options for maximizing energy generation are: applying (PV41) with a fixed skylight on the roof, (PV27) on the solid wall of eastern facade, and/or (PV41) on the glass of southern and western facades. The best economic options are: applying (PV27) on the solid roof, the southern shading devices, and the western solid wall.

The method is flexible and powerful for building designers and engineers to enhance their buildings with BIPV options, by comparing and selecting optimized alternatives and the most matching PVs based on their priorities. In addition, the method can principally include more building envelope options and parameters such as window-to-wall ratio (WWR), locations of windows and so on. Minimizing the whole building energy consumption can be included instead of purely maximizing the PV generation as a rigorous optimization objective for the method. Architectural creativity can/will also be considered to reach an esthetically unique and meaningful 3D architectural massing such as using measurable architecture principles. Shape grammar rules can be used for generating different shapes and geometries from an initial model. A computational tool will eventually be developed based on the proposed framework and its extensions.

Acknowledgements

The authors would like to acknowledge the financial support of the Egyptian Ministry of Higher Education for this research.

Appendix

The collected PV modules to be used in the model application (this table was built based on information collected from websites of related manufacturers)

PV Number	PV module name and type			PV module characteristics								Energy performance					PV cost	
					Dimensions								Absolute generated energy (W)		Generated energy (W/m²)			
	Brand name	PV type	Classification (BIPV/ opaque)	Weight (kg)	Width (m)	Length (m)	Area (m²)	Color	Flexibility (Yes/ foldable (F)/No)	Reflection (Yes/semi (S)/No)	Transparency (%)	Module (%)	Average	Maximum	Average	Maximum	Total capital cost ($)	Cost ($/(W·yr))
PV1	LA130-24S	Mono	Opaque	10.5	63.6	143	0.91	Black	No	No	0	18.5	112	132	123	145	743.7	0.23
PV 2	LA50-12S	Mono	Opaque	5.2	52.7	69.6	0.37	Black	No	No	0	18.5	42.5	50	116	136	291.4	0.23
PV 3	LA-20-12S	Mono	Opaque	1.2	29	58.5	0.17	Black	No	No	0	18.5	17	20	100	118	124.3	0.25
PV 4	Sunlight Well SW6F-280W	P–Si	Opaque	22.3	98.2	195	1.92	Dark blue	No	No	0	14.6	217	280	113	146	1431	0.20
PV 5	Sunlight Well SW125M-250W	Mono	Opaque	20	106	160	1.7	Black	No	No	0	14.7	194	250	114	147	1234	0.20
PV 6	Sunlight Well S125M-180W	Mono	Opaque	15.5	80.8	158	1.28	Black	No	No	0	14.1	140	180	109	141	878.9	0.20
PV 7	Sunlight Well S156P-120W	P–Si	Opaque	10.5	66.9	134	0.89	Dark blue	No	No	0	13.4	93	120	104	134	541.8	0.18
PV 8	Sunlight Well SW-2W	P–Si	Opaque	0.8	20	24	0.05	Dark blue	No	No	0	14.6	3.1	4	64.6	83.3	24.7	0.25
PV 9	LONG ENERGSLSM-230P	P–Si	Opaque	19.5	99.5	164	1.63	Blue	No	No	0	17.5	178	230	109	141	1592	0.28
PV10	LONG ENERGYSLSM-205D	Mono	Opaque	16.5	80.8	158	1.28	Black	No	No	0	18.5	159	205	124	161	1417	0.28
PV11	QJP-Module 300W	P–Si	Opaque	23.1	99.2	196	1.94	Dark blue	No	No	0	16.5	233	300	120	155	1244	0.17
PV12	QJP-Module 215W	P–Si	Opaque	19.5	99.2	164	1.63	Dark blue	No	No	0	16.5	167	215	102	132	891.7	0.17
PV13	QJP-Module 175W	P–Si	Opaque	19	99.2	148	1.47	Blue	No	No	0	16.5	136	175	92.3	119	1902	0.43
PV14	QJM-Module 85W	Mono	Opaque	8.4	55.2	120	0.66	Black	No	No	0	18.5	65.9	85	99.4	128	352.5	0.17
PV15	TLT-200WMC8	Mono	Opaque	19	99	148	1.47	Black	No	No	0	13.5	155	200	106	137	903	0.18
PV16	TLT-140W-6P36 SPEC	P–Si	Opaque	12	67	148	0.99	Dark blue	No	No	0	15.5	109	140	109	141	632.1	0.18
PV17	TLT-90W-SPEC	Mono	Opaque	8.5	54	120	0.65	Black	No	No	0	15.5	69.8	90	108	139	419.9	0.19
PV18	TLT-50W SPEC	P–Si	Opaque	5.3	61	67	0.41	Dark blue	No	No	0	15.5	38.8	50	94.8	122	255.9	0.20
PV19	TLT-15W-SPEC	Mono	Opaque	2.4	29	45	0.13	Black	No	No	0	15.5	11.6	15	89.1	115	70	0.19
PV20	JHMM-120W	Mono	Opaque	10.5	68	148	1.01	Black	No	No	0	14.2	93	120	92.4	119	1174	0.39
PV21	HP-185	Mono	Opaque	16	80.8	158	1.28	Black	No	No	0	14.5	143	185	112	145	333	0.07
PV22	HP-100	Mono	Opaque	9.62	80.8	103	0.83	Dark blue	No	No	0	12	77.5	100	93.1	120	177.5	0.07
PV23	HP-10	Mono	Opaque	1.25	29.3	34.5	0.1	Black	No	No	0	11	7.75	10	76.7	98.9	17.5	0.07
PV24	LNSF 295P	P–Si	Opaque	23	99.2	195	1.93	Dark blue	No	No	0	16.5	215	295	111	153	219	0.03
PV25	LNSE 240P	P–Si	Opaque	20	99.2	164	1.63	Blue	No	No	0	14.9	176	240	108	148	178.2	0.03
PV26	LNSE 180P	Mono	Opaque	15.5	80.8	158	1.28	Black	No	No	0	18.5	130	180	102	141	133.7	0.03
PV27	LB300QM-72	Mono	Opaque	27	99.2	196	1.94	Black	No	No	0	18.5	233	300	120	155	177	0.02
PV28	LB230QM-60	Mono	Opaque	19.5	99.1	165	1.64	Black	No	No	0	14.1	178	230	109	141	135.7	0.02
PV29	Amplesun	A–Si	Opaque	20.3	110	140	1.54	Black	No	No	0	7.5	77.5	100	50.3	64.9	67.5	0.03
PV30	Amplesun	Mono	Opaque	20.3	111	141	1.58	Dark brown	No	No	0	17	77.5	100	49.2	63.5	130	0.05
PV31	SC280P-24	P–Si	Opaque	24	99.2	196	1.94	Dark blue	No	No	0	16	272	280	140	144	480.2	0.07
PV32	SC240M-24	Mono	Opaque	16.8	108	158	1.71	Black	No	No	0	18.5	232	240	136	141	403	0.07
PV33	SC35M-12	Mono	Opaque	4.2	53.7	61.7	0.33	Blue	No	No	0	18.5	34	35	103	106	65.88	0.08
PV34	SC25M-12	Mono	Opaque	3.1	44.7	53.7	0.24	Dark blue	No	No	0	18.5	24.3	25	101	104	40.63	0.07
PV35	DSP300M	Mono	Opaque	23	99.2	196	1.94	Black	No	No	0	18.5	291	300	150	155	277.5	0.04
PV36	DSP180P	P–Si	Opaque	15.6	80.8	158	1.28	Blue	No	No	0	16.5	175	180	137	141	90	0.02
PV37	DSP80M	Mono	Opaque	8.2	55	120	0.66	Black	No	No	0	18.5	77.6	80	118	121	58	0.03
PV38	DSP50M	Mono	Opaque	8	54.2	71	0.38	Black	No	No	0	18.5	48.5	50	126	130	45	0.04
PV39	Power World PW100A	A-Si thin film	BIPV(2 Glass)	18	110	130	1.43	Black	No	S	20	7.5	90	100	62.9	69.9	70.2	0.03
PV40	Power World PWBIPV180	Mono	BIPV (on glass)	45	100	170	1.7	Dark blue	No	S	40	17.8	140	180	82.1	106	256.5	0.06
PV41	Power World PW190-72	Mono	BIPV (on glass)	16	80.8	158	1.28	Black	No	S	40	17.8	147	190	115	149	266	0.06
PV42	Shine SN-H130W	Mono	BIPV (sheets)	2	54	144	0.77	Dark blue	Yes	S	0	20	101	130	130	168	260	0.08
PV43	Shine SN-H120W	Mono	BIPV (sheets)	1.8	54	131	0.7	Black	Yes	S	0	20	93	120	132	170	150	0.05
PV44	Shine SN-H30W	Mono	BIPV (sheets)	–	37.8	53.5	0.2	Dark blue	Yes	S	0	20	23.3	30	115	148	37.5	0.05
PV45	Solar First-SFM60W	Mono	Sheets	–	55	90	0.5	Dark blue	Yes	No	0	18.5	46.5	60	93.9	121	102	0.07
PV46	SolarFirst-Semi flexible	Mono	BIPV (sheets)	–	80	106	0.85	Black	Yes	No	0	20	93	120	110	142	204	0.07
PV47	Bluesun	Mono	BIPV (2 Glass)	–	100	100	1	Any	No	S	20	20	93	120	93	120	90	0.03
PV48	Bluesun - DDM 1090X	Triple junction	Opaque (CPV)	56.4	108	174	1.88	Transparent	F	S	0	28	349	450	186	239	3007	0.27
PV49	Bluesun - B240P60	P–Si	Opaque	19.5	99.2	165	1.64	Dark blue	F	No	0	16.5	186	240	114	147	120	0.02
PV50	X-greenpower	A–Si thin film	BIPV (sheets)	–	14	19.5	0.03	Any	Yes	No	0	8	1.16	1.5	42.6	54.9	13.05	0.35
PV51	X-greenpowe–GSB97	A–Si thin film	Opaque	25.5	110	140	1.54	Black	No	No	0	7.5	97	103	63	66.9	108.2	0.04
PV52	X-greenpower–XF144	A–Si thin film	BIPV (Strips)	7.7	39.4	548	2.16	Dark blue	Yes	No	0	7.5	104	144	48.2	66.7	460.8	0.13
PV53	X-greenpower–XF68	A–Si thin film	BIPV (Strips)	–	39.4	285	1.12	Pink	Yes	No	0	7.5	52.7	68	46.9	60.6	217.6	0.13
PV54	Hilight Solar-HSA40WP	A–Si thin film	Opaque	14.4	63.5	125	0.79	Dark gray	No	S	0	6.3	77.5	100	98	126	116.5	0.05
PV55	Hilight Solar-HSA85WP	A–Si thin film	Opaque	28.3	110	140	1.54	Dark blue	No	S	0	6	65.9	85	42.8	55.2	99	0.05
PV56	Hilight Solar-HSA25WP	A–Si thin film	Opaque	5	39.5	125	0.49	Puce	No	S	0	5	19.4	25	39.2	50.6	37.5	0.06
PV57	Hilight Solar-HSA100WP	A–Si thin film	Opaque	18	111	131	1.45	Black	No	S	0	7.3	77.5	100	53.4	68.9	89	0.04

(Continued)

PV58	UNISOLAR - PVL68	A–Si thin film	BIPV (Strips)	3.9	40	185	0.74	Dark blue	Yes	S	0	7.5	52.7	68	71.2	91.9	289	0.17
PV59	LQPVL	A–Si thin film	BIPV (Strips)	7.5	39.4	549	2.16	Dark blue	Yes	No	0	7.5	136	144	62.9	66.6	576	0.16
PV60	Ganghang	Mono / poly	BIPV (on glass)	–	52.7	104	0.55	Any	No	S	5	–	63.9	82.5	117	151	162.8	0.08
PV61	Ganghang	Mono / poly	BIPV (on glass)	–	52.7	104	0.55	Any	No	S	30	–	46.9	60.5	85.8	111	162.8	0.11
PV62	Ganghang	Mono / poly	BIPV (on glass)	–	52.7	104	0.55	Any	No	S	60	–	29.8	38.5	54.6	70.4	162.8	0.17
PV63	SYFD - SYFD75W	Mono	BIPV (sheets)	–	53.5	82	0.44	Dark blue	Yes	S	0	21	58.1	75	132	171	115	0.06
PV64	SYFD - SYFD100W	Mono	BIPV (sheets)	–	54	105	0.57	Dark blue	Yes	S	0	21	77.5	100	137	176	115	0.05
PV65	FY-BIPV150W	Any	BIPV (on glass)	–	100	100	1	Any	No	S	5	–	116	150	116	150	300	0.08
PV66	FY-BIPV80W	Any	BIPV (on glass)	–	100	100	1	Any	No	S	50	–	62	80	62	80	300	0.15
PV67	FY-BIPV120W	Any	BIPV (on glass)	–	100	100	1	Any	No	S	25	–	93	120	93	120	300	0.10

References

Albere AG (2009). Thin-film solar cells. *Thin Solid Films*, 517: 4706–4710.

AM Soalr (2014). Standard Test Conditions (STC) vs. Normal Operating Cell Temperature (NOCT). Available at http://www.amsolar.com/home/amr/page_164. Accessed 20 Oct. 2014.

ASHRAE (2007). ANSI/ASHRAE/IESNA Standard 90.1-2007. Final Qualitative Determination. Atlanta: ASHRAE.

Autodesk (2014). Ecotect Analysis Software Homepage. Available at http://usa.autodesk.com/ecotect-analysis. Accessed 20 Oct. 2012.

BaicheB, Williams N (2001). Architect's Data, 3rd edn. Hoboken, USA: Blackwell Science.

Capeluto G, Yezioro A, Bleiberg T, Shaviv E (2005). From computer models to simple design tools: Solar rights in the design of urban streets. In: Proceedings of 9th IBPSA International Conference, Montreal, Canada.

Carmody J, Selkowitz S, Lee ES, Arasteh D, Willmert T (2004). Window Systems for High Performance Commercial Buildings. London: W. W. Norton & Company.

Choudhary R, Augenbroe G, Gentry R, Hu H (2008). Simulation-enhanced prototyping of an experimental solar house. *Building Simulation*, 1: 336–355.

DOE-2 (2014). DOE-2 Based Software Homepage, eQuest. Available at http://www.doe2.com/equest. Accessed 20 Oct. 2014.

EIA (2013). International Energy Statistics, Electricity Generation. Available at http://www.eia.gov/tools/faqs. Accessed 16 Oct. 2014.

Gips J (2012). Shape grammars. Available at http://www.shapegrammar.org. Accessed 20 Oct. 2014.

Gumm M (2008). Integrating photovoltaics onto building envelope surfaces. Available at http://www.mrca.org/ technical/pv-project. Accessed 16 Oct. 2014.

Harvey LDD (2009). Reducing energy use in the buildings sector: Measures, costs and examples. *Energy Efficiency*, 2: 139–163.

Henemann A (2008). BIPV: Built-in solar energy. *Renewable Energy Focus*, 9:14–19.

Hwang T, Kang S, Kim JT (2012). Optimization of the building integrated photovoltaic system in office buildings–Focus on the orientation, inclined angle and installed area. *Energy and Buildings*, 42: 92–104.

Jin JT, Cho HJ, Jeong JW (2012).Optimization of freeform building shape using genetic algorithm. In: Proceedings of 1st IBPSA Asia Conference (ASim2012), Shanghai, China.

Kampf JH, Robinson D (2010). Optimization of building form for solar energy utilization using constrained evolutionary algorithms. *Energy and Buildings*, 42: 807–814.

Karaguzel OT, Zhang R, Lam KP (2014). Coupling of whole-building energy simulation and multi-dimensional numerical optimization for minimizing the life cycle costs of office buildings. *Building Simulation*, 7: 111–121.

Kho J (2010). Pretty and efficient, concentrating PV. Available at http://www.pv-magazine.com/archive/articles/beitrag/pretty-and-efficient. Accessed 16 Oct. 2014.

Ly P, Ban-Weiss G, Finch N, Wray C, De Ogburn M, Delp W, Akbari H, Smaby S, Levinson R, Gean B (2013). Building integrated photovoltaic (PV) roofs for sustainability and energy efficiency. Washington, DC: Navac Facilities Engineering Command (NAVFAC), Engineering & Expeditionary Warfare Center (EXWC).

Prasad DK, Snow M (2005). Designing with solar power—A sourcebook for building integrated photovoltaics (BIPV). Melbourne: Images Publishing.

Tuhus-Dubrow D, Krarti M (2010). Genetic-algorithm based approach to optimize building envelope design for residential buildings. *Energy and Buildings*, 45: 1574–1581.

Ministry of Electricity and Energy (2011). Annual Report. Cairo, Egypt: Ministry of Electricity and Energy.

NRCAN (2014). Natural Resources Canada, RETScreen International. Available at http://www.retscreen.net/ang/home.php. Accessed 20 Oct. 2014.

NREL (2014). System Advisor Model, SAM. Available at https://sam.nrel.gov. Accessed 20 Oct. 2014.

Open Studio (2014). OpenStudio 1.5.0 Release. Available at https://www.openstudio.net. Accessed 20 Oct. 2014

SFA (2013). Solar facts and advice, thin film technology survey. Available at http://www.solar-facts-and-advice.com/thin-film.html. Accessed 16 Oct. 2014.

Sui J, Munemoto J (2007). Shape study on a green roof integrated photovoltaic system for bi-objective optimization of investment value and CO_2 emission. *Asian Architecture and Building Engineering*, 6: 307–314.

Suna D, Polo A L, Haas R (2006). Demand Side Value of PV. Vienna: Vienna University of Technology.

Topaloğlu B (2003). Solar envelope and form generation in architecture. Master Thesis, Middle East Technical University, Turkey.

You W, Qin M, Ding W (2013). Improving building facade design using integrated simulation of daylighting, thermal performance and natural ventilation. *Building Simulation*, 6: 269–282.